

# High resolution spectroscopy in gases and its application on the frequency stabilization of semiconductor lasers

E. de Carlos López<sup>a,b</sup> and J.M. López Romero<sup>a</sup>

<sup>a</sup>*División de Tiempo y Frecuencia, CENAM*

*Km. 4.5 Carretera a los Cués, el Marqués Qro., C. P. 76900, México.*

<sup>b</sup>*Facultad de Ciencias, UAEM*

*Avenida Universidad no. 1001, Colonia Chamilpa, Cuernavaca Mor., C. P. 62210, México.*

*e-mail: edlopez@cenam.mx, jlopez@cenam.mx*

Recibido el 11 de agosto de 2003; aceptado el 4 de marzo de 2004

The gas spectroscopy is a standard technique for frequency stabilization in semiconductor lasers. The Doppler effect is what exerts most influence on the linewidths of atomic spectrum increments. In the present work, the saturation spectroscopy, whose main characteristic is to cancel the undesirable consequences of this effect, is studied. Different techniques of dispersion-like signals generation are revised, and are used as error signals in the stabilization of semiconductor lasers. From a different point of view, these techniques are reviewed and being compared. Moreover, the experimental results of Cesium 133 spectroscopy made at Centro Nacional de Metrología, CENAM, are exhibited herein.

*Keywords:* Saturation spectroscopy; semiconductor laser stabilization.

La espectroscopia en gases es una de las técnicas más utilizadas en la estabilización en frecuencia de láseres semiconductores. El efecto Doppler es el factor que más influye en el ensanchamiento de las líneas de los espectros atómicos. En este trabajo se revisa la espectroscopia de saturación, cuya característica principal es la de anular las consecuencias indeseables de este efecto. Se examinan distintas técnicas de generación de señales tipo dispersión, las cuales son empleadas como señales de error en la estabilización de láseres semiconductores. Estas técnicas se comparan entre sí y son revisadas desde una perspectiva diferente a lo que convencionalmente se presenta en la literatura. Asimismo se muestran resultados experimentales de espectroscopia en gas de Cesio 133 realizadas en el Centro Nacional de Metrología, CENAM.

*Descriptores:* Espectroscopia de saturación; estabilización de láseres semiconductores.

PACS: 32.70.Jz; 42.55.Px; 05.20.Dd

## 1. Introduction

Many applications of semiconductor lasers, require, high stability and minimal frequency dispersion. In the research field, the cooling neutral atoms experiments [1,2], The Bose-Einstein condensation [3], and the development of atomic lasers [4] are some of the most recent examples of the application of stabilized lasers, particularly of semiconductor lasers.

Frequency stabilization of semiconductor lasers requires a good control of the parameters that affect the emission characteristics, being temperature and feeding current two of the most important ones. However, for some applications, highly stable current sources and temperature control are not enough by themselves, being necessary to use frequency references of a very good quality such as resonance cavities and atomic or molecular systems. Some of the best frequency references are atomic transitions. In this context, spectroscopy has become a valuable tool, not only for the study of atomic structure, but also for building extremely stable frequency references [5].

In Sec. 2 of this paper, saturation spectroscopy [6,7] is revised, because it has the characteristic that suppresses the undesired Doppler effects in the resonance spectrums. On the 3rd section, different techniques to generate the dispersion-

like signals being used to stabilize semiconductor lasers are exposed. As well as some experimental results obtained with gas of Cesium 133 in the laboratories of Centro Nacional de Metrología, CENAM, are presented. The discussion of the results and the revision of the different techniques to generate dispersion-like signals are seen from a different point of view from those usually reported in science literature.

## 2. Saturation spectroscopy

### 2.1. Saturation spectroscopy for an ideal gas, composed by atoms with three discrete energy levels

As the atoms or molecules that compose a gas are in movement due to the temperature conditions, the radiation emitted or absorbed by them will have a frequency shift due to the Doppler effect. The width of the lines of the spectrums obtained are then increased by this effect, as the frequency of the radiation emitted or absorbed depends on the atomic or molecular speeds. A good way to suppress the undesired consequences of this effect is using the so-called saturation spectroscopy. In this technique, two overlapped light beams, which propagate in opposite directions and with the same frequency  $\omega$ , are used close to the atomic resonance. Figure 1

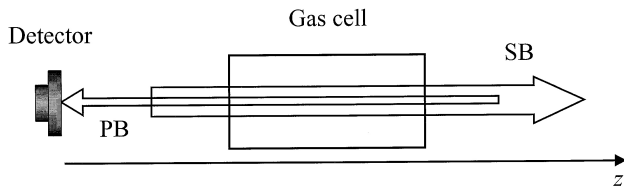


FIGURE 1. Saturation spectroscopy experimental set up. SB is the Saturation Beam and PB is the Probe Beam.

shows, graphically, the experimental implementation of this technique.

The gas in the container, shown in Fig. 1, is considered to be an ideal monatomic gas in thermodynamic equilibrium at a temperature  $T$ . Let us suppose that the atoms that compose that gas have only three discrete non-degenerated energy states: levels  $a$ ,  $b$ , and  $c$ , where  $a$  is the ground state, while  $b$  and  $c$  are the excited states, with energies  $E_a$ ,  $E_b$ ,  $E_c$ , respectively, and  $E_a < E_b < E_c$ ; and that the only permitted transitions with a single photon are  $a \rightarrow b$ , and  $a \rightarrow c$ , and these have an energy difference  $E_b - E_a = \hbar\omega_2$  and  $E_c - E_a = \hbar\omega_1$ , being  $\hbar\omega_1 > \hbar\omega_2$ . Additionally, let's consider that both transitions have the same probability to be achieved.

In case the light beams propagate through the  $z$  axis (Fig. 1), the atoms that have a  $z$  velocity component given by  $v_z^r(\omega_1) = (\omega - \omega_1)/k$ , and  $v_z^r(\omega_2) = (\omega - \omega_2)/k$  are the ones that have a higher probability to interact with light beams. It is easy to find, from the analysis of the velocity distribution on the component  $z$  for the population of atoms on the ground state  $dN_a/dv_z$ , that four holes are generated due to the interaction with the light beams, as shown in Fig. 2a. Such holes are originated due to the portion of atoms that leave the  $a$  state to populate a higher state.

Considering that a continuous change in the frequency of the light beams from  $\omega > \omega_1, \omega_2$  to  $\omega < \omega_1, \omega_2$  happens, the holes move in opposite directions causing three overlaps among them. The first one happens in the center of the velocity distribution, where  $v_z^r(\omega_1) = 0$ , and, it is only produced when the condition  $\omega = \omega_1$  is reached. Then a double overlap appears in the point  $\pm v_z^r(\omega_1) = \mp v_z^r(\omega_2)$ , it means, when  $\omega$  has the value of  $(\omega_1 + \omega_2)/2$ . Finally, the third overlap is done in the central part of the distribution where  $v_z^r(\omega_2) = 0$ , under the condition  $\omega = \omega_2$ . Figure 2 shows this sequence.

On condition that the holes overlap in the central part of the distribution, the frequency  $\omega$  of the laser is the same as the resonance frequency  $\omega_1$  or  $\omega_2$ . This way, the atoms that interact with the light are those that move in a perpendicular plane to the direction of the propagation of the laser. The light beam that moves from left to right (Fig. 1), known as saturation beam, induces the transition of the atoms that move in such plane to an excited state. The beam that moves in opposite direction to the saturation beam, called probe beam (usually of lower power than the saturation beam), will find its way with these same atoms in an excited state, so that this beam will not be able to interact with them.

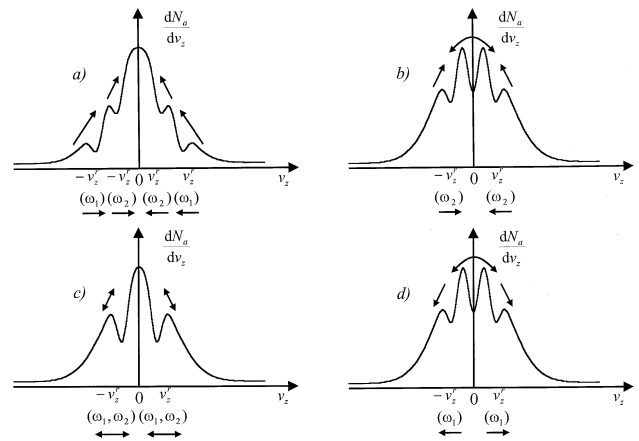


FIGURE 2. Dynamic of holes in the velocity distribution of the  $z$  component and  $a$  state. This case is for a fictitious atom with two transitions.

On the other hand, when the angular frequency  $\omega$  gets the value of  $(\omega_1 + \omega_2)/2$ , the atoms with a velocity component in  $z$  axis equal to  $v_z = \pm v_z^r(\omega_1, \omega_2) = \pm(\omega_1 - \omega_2)/2k$  are the only ones that will interact with the light beams. When we make an analysis of the process of interaction of a photon with an atom, in the non relativistic regime, we obtain [8]:

$$\Delta E = \hbar\omega - \hbar\mathbf{v} \cdot \mathbf{k}, \tag{1}$$

where  $\Delta E$  represents the difference of energy among the discrete atom states. For the case being considered, it could be that  $\Delta E = E_b - E_a$  or  $\Delta E = E_c - E_a$ .

When  $v_z = +v_z^r(\omega_1, \omega_2) = +(\omega_1 - \omega_2)/2k$ , the equation (1) happens to be  $\Delta E = \hbar\omega_2$ , it is, the atom makes the transition  $a \rightarrow c$ . For  $v_z = -v_z^r(\omega_1, \omega_2) = -(\omega_1 - \omega_2)/2k$ , the difference of energy is  $\Delta E = \hbar\omega_1$ , it is, the atom makes the transition  $a \rightarrow b$ . In other words, if the velocity component  $v_z = v_z^r(\omega_1, \omega_2)$  of the atom is in opposite direction to the direction of the laser propagation, the atoms make the transition  $a \rightarrow c$ . Note that the missing energy is compensated by the Doppler effect. On the other hand, if the velocity component is in the same direction than the one of the laser propagation, then the atoms make the transition  $a \rightarrow b$ , it is, the surplus energy is also compensated by the Doppler effect.

The spectrum obtained is shown in the Fig. 3. Such spectrum show the transmitted intensity,  $S(\omega)$ , in the probe beam. The shape of the well in the spectrum is partially related with the distribution of the speeds of the atoms that form the gas, and it is known as Doppler well. Additionally to it, three peaks appear, called Lamb dips, two of which are located in  $\omega_1$  and  $\omega_2$ , meanwhile the third one is in  $(\omega_1 + \omega_2)/2$ . The origin of these three Lamb dips is the result of the intensity increment of the light transmitted, due to the no-interaction of the probe beam with the gas, as it was explained previously. It is important to explain that the presence of the Doppler well induces a systematic effect in the location of the Lamb dips, so that actually there is a very low deviation of those compared with atomic transitions. In the same way, the sym-

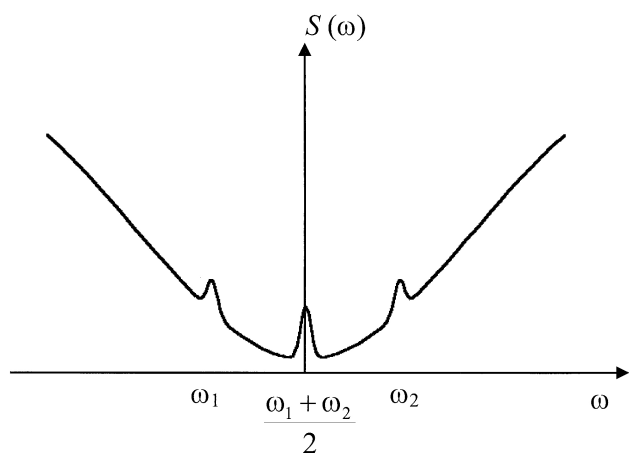


FIGURE 3. Graphic of transmitted light intensity as function of frequency  $\omega$ . The crossover line is at the middle of  $\omega_1$  and  $\omega_2$ .

metry of this signal is due to the supposition that the atomic transitions have the same probability to appear.

When Fig. 2c is observed, it can be noticed that there are two simultaneous overlaps in the velocity distribution. Making a statistic interpretation of this fact, it is inferred that the number of atoms that make any transition when  $\omega = (\omega_1 + \omega_2)/2$  is higher for the cases on which  $\omega = \omega_1$  and  $\omega = \omega_2$  (see Figs. 2b and 2d). For this reason, the Lamb dip associated to  $\omega = (\omega_1 + \omega_2)/2$  is the most prominent. This Lamb dip that appear additionally in the atomic spectrum is known as of crossover line. These crossover lines appear just at the central point between each pair of Lamb dips corresponding to real transitions. In the case of a gas, composed by atoms with three permitted transitions, the spectrum will have three Lamb dips due to real transitions, and three crossover lines, one for each pair of transitions. An example of this kind of spectrums will be seen in the following section, where some experimental results of the application of saturation spectroscopy with Cesium-133 gas, are also shown.

## 2.2. Saturation spectroscopy in Cs-133: experimental results

One of the most used alkaline elements in Atomic Physics is Cesium 133. In Metrology, this element has particular relevance because of the unit of time, the second of the International System of units. The unit of time is defined in terms of the hyperfine levels of the Cs-133 ground state [9]. In Fig. 4 are shown the first energy levels of this atom.

The experimental measurements of the resonance spectrums of the Cs-133 D2 line reported in this paper, were obtained by using a semiconductor DBR type laser, with 5 mW output power (Yokogawa, model YL85XTW). The wavelength of the radiation emission of this laser is near to the D2 Cs-133 line (852 nm), it is the  $|6^2s_{1/2}\rangle \rightarrow |6^2p_{3/2}\rangle$  transition, near infrared. The frequency dispersion (linewidth of the emitted radiation) of the laser is around 1 MHz. The laser, and its DBR section, were fed with a highly stable electric

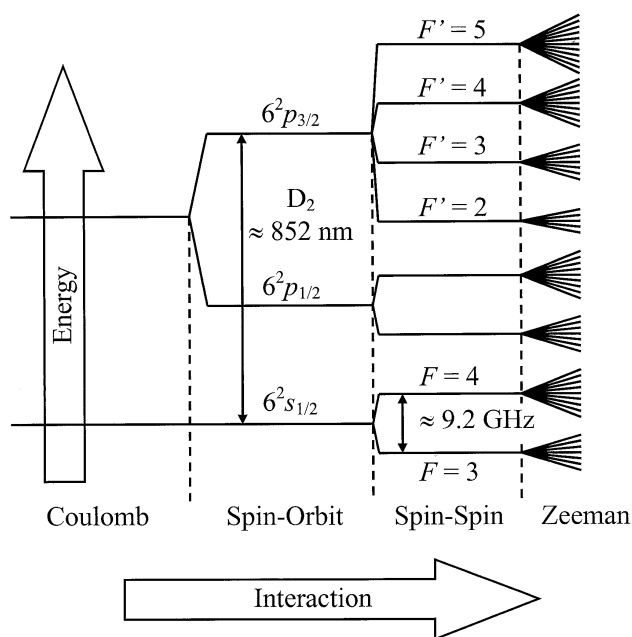


FIGURE 4. First Cesium-133 energy levels.

current source. The current stability was better than  $\pm 1 \mu\text{A}$  per hour. Nominal values for laser and DBR current were 40 mA and 20 mA, respectively.

On the other hand, the laser temperature was maintained around room temperature (22 °C) in order to keep the resonant condition. Temperature control at the laser was achieved by using a PID control along with a Peltier thermo cooler element. The temperature stability was better than  $\pm 1$  mK per hour. The frequency of the laser was modulated around the  $|6^2s_{1/2}, F=3\rangle \rightarrow |6^2p_{3/2}, F'=2, 3, 4\rangle$ , and  $|6^2s_{1/2}, F=4\rangle \rightarrow |6^2p_{3/2}, F'=3, 4, 5\rangle$  transitions. It was achieved through the modulation of the DBR current by using a 100 Hz triangle signal. The Cs-133 was contained in a cubic cell (1 cm  $\times$  3 cm  $\times$  1 cm), and its temperature was kept around 23 °C with a vapour pressure near  $10^{-6}$  torrs [10]. The power of both, the saturation and probe beams were of 80  $\mu\text{W}$  and 20  $\mu\text{W}$ , respectively. Polarization in both laser beams was linear. Diameter of the laser beams was near 1.5 mm. The thinner part of the cell was used to pass through both laser beams. In Fig. 5, we show the experimental set up where measurements were made. In Fig. 6, we show the spectrums obtained with this set up.

Spectrums in Fig. 6 are taken from an oscilloscope fed with the photodetector signal. Figure 6 also shows the triangular signal used in order to achieve the frequency modulation in the laser beams. The positive slope in such triangular signal corresponds to an increment of the DBR electric current, and also producing an increment on the laser wavelength emission. Moving to the right side inside the Doppler well, we will find Lamb dips corresponding to less energetic transitions. So, the extreme right side Lamb dip in the spectrum corresponds to the lowest energetic transition, and the extreme left side Lamb dip corresponds to the most energetic

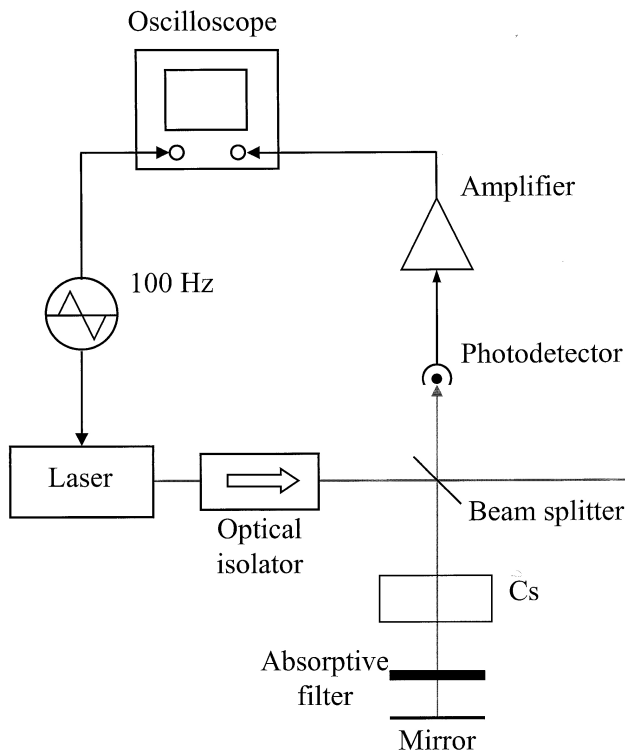


FIGURE 5. Cesium-133 saturation spectroscopy experimental set up.

resonance. In Fig. 6b appear 6 Lamb dips inside the Doppler well, three of them corresponding to three real atomic transitions and the other three correspond to the crossover lines. However, in Fig. 6a appear five Lamb dips clearly formed and one partially formed. This is because the laser has a mode hop on its frequency emission just at the position of the crossover line appearing just at the middle part of the  $|6^2s_{1/2}, F = 3\rangle \rightarrow |6^2p_{3/2}, F' = 3\rangle$ , and  $|6^2s_{1/2}, F = 3\rangle \rightarrow |6^2p_{3/2}, F' = 2\rangle$  transitions.

It is interesting to notice the asymmetry on the spectrums in contrast to the symmetry presented on section 2.1 (see Fig. 3). Such asymmetries are caused because the involved transitions do not have the same relative transition probability. As an example, in the spectrum shown in Fig. 6b the  $|6^2s_{1/2}, F = 4\rangle \rightarrow |6^2p_{3/2}, F' = 5\rangle$  transition Lamb dip is at the bottom of the Doppler well, indicating that such transition is the most probable transition. On the other hand, the  $|6^2s_{1/2}, F = 4\rangle \rightarrow |6^2p_{3/2}, F' = 3\rangle$  transition Lamb dip is at the top part of the Doppler well, indicating that such transition has the lowest transition probability.

### 3. Frequency stabilization of semiconductor lasers

A relevant characteristic of the semiconductor lasers is that their frequency of emission changes as a function of their temperature and circulating electric current. By this reason, it is very important to have a good control on such parameters in order to stabilize the frequency. As an example, we could

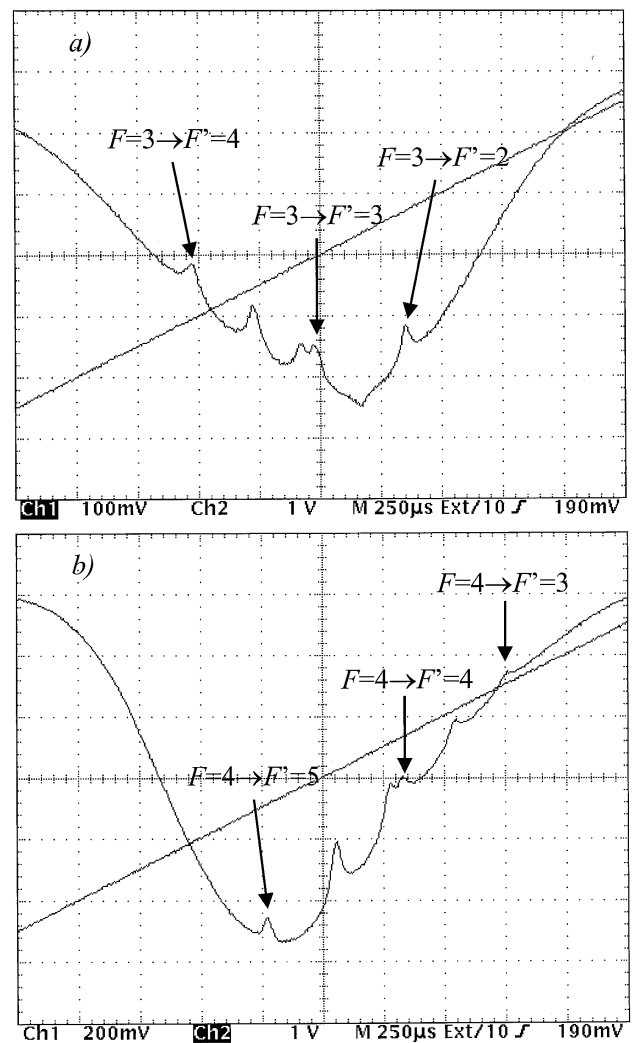


FIGURE 6. Cesium-133 hyperfine resonance spectrums. a) Spectrum of  $|6^2s_{1/2}, F = 3\rangle \rightarrow |6^2p_{3/2}, F' = 2, 3, 4\rangle$  transitions. b) Spectrum of  $|6^2s_{1/2}, F = 4\rangle \rightarrow |6^2p_{3/2}, F' = 3, 4, 5\rangle$  transitions.

say that it is common to find that the wavelength of the emission of a semiconductor laser has an electric current sensitivity coefficient of around 0.01 nm/mA, and for each Kelvin its wavelength changes around 0.1 nm. In this particular case of the semiconductor lasers with emission around 852 nm, the frequency shifts are of the order of magnitude of 4 GHz and 40 GHz, respectively.

Usually semiconductor lasers have linewidths with large frequency dispersion, which are of the order of magnitude of around  $10^8$  Hz, very often higher than the atomic transition line width. With the purpose to resolve the atomic transitions resonance, it is necessary to add an element in order to decrease the laser linewidth. Such element could be part of the semiconductor, in the DBR (Distributed Bragg Reflector) type diode lasers, or the DBF (Distributed Feedback) type diode lasers [11]. It is also possible to find them as external elements, that is the case of the resonant extender cavities or

the diffraction gratings [12]. Such elements are very often used to control the emission frequency of the laser too.

In order to stabilize the emission of a semiconductor laser to an atomic line, it is necessary to use an electronic servo loop to keep the frequency radiation of the laser in resonance with the atomic transition frequency. Such servo loop must be fed with a signal containing information about the resonance frequency. Figure 3 shows signals that could be used to feed the servo loop. The electronic circuitry of the servo loop keeps the laser emitting in resonance with the frequency, where the maximum of a selected Lamb dip in the spectrum is located. The maximums are located using the relative of the spectrums, the result is a signal known as a dispersion-like signal which is used as error signal to feed the servo loop. In the next section, we review briefly some of the most used methods to generate the dispersion-like signals, and we also show some experimental results of hyperfine spectroscopy on Cs-133 vapour.

### 3.1. Modulated frequency spectroscopy

Supposedly the emission frequency of the laser  $\omega(t)$  is slightly modulated around a frequency  $\omega'$ , in this case we can write:

$$\omega(t) = \omega' + A_\omega \sin(\omega_m t), \quad (2)$$

where  $\omega_m$  is the modulation frequency and  $A_\omega$  is the modulation deep. If the modulation deep  $A_\omega$  is much smaller than the transition linewidth, then the transmitted intensity  $S(\omega)$  could be written approximately as:

$$S(t) = S(\omega') + \frac{d}{d\omega} S(\omega)|_{\omega=\omega'} A_\omega \sin(\omega_m t). \quad (3)$$

On the other hand, if the signal  $S(t)$  is multiplied by the modulation signal  $\sin(\omega_m t)$ , and then it is used a low pass filter in order to eliminate all the time dependent terms, it is obtained:

$$\text{Lowpass}[S(t) \sin(\omega_m t)] = \frac{A_\omega}{2} \frac{d}{d\omega} S(\omega) \Big|_{\omega=\omega'}, \quad (4)$$

which is the error signal that could be used to feed the servo loop in order to stabilize the laser.

### 3.2. Spectroscopy with frequency modulation in Cs-133

An experimental set up used to perform hyperfine spectroscopy in Cs-133 using a frequency modulation technique is shown in Fig. 7. The conditions on the Cs cell were the same as those described in Sec. 2.2. The power of saturation and probe laser beams were  $300 \mu\text{W}$  and  $75 \mu\text{W}$ , respectively. The increased power on the laser beams was adopted in order to have a better signal-to-noise ratio on the dispersion-like signal.

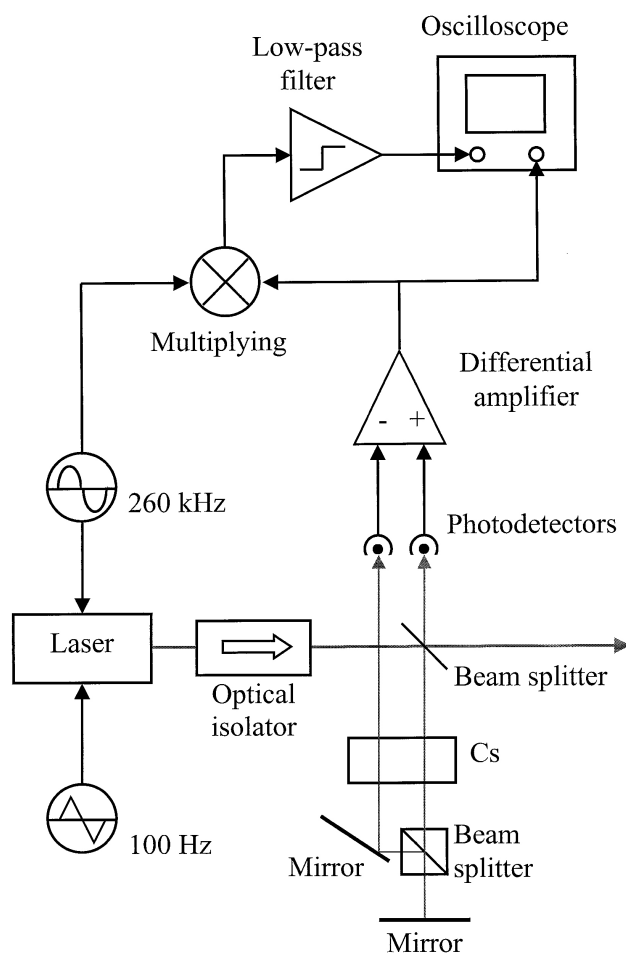


FIGURE 7. Schematics of the experimental set up using FM spectroscopy with Cesium-133.

The high frequency modulation (see equation 2) was created using a sinusoidal signal of 260 kHz, fed directly on the laser (phase control pin). The low frequency modulation was achieved in the same way as described in Sec. 2.2. Figure 8 shows the results obtained with this technique. Spectrum in Fig. 8 corresponds to the transitions  $|6^2s_{1/2}, F=4\rangle \rightarrow |6^2p_{3/2}, F'=3, 4, 5\rangle$ . The set up was designed in order to subtract the Doppler well from the spectrums, see Fig. 6. This was done with the aim to minimize the systematic error on the position of the Lamb dips. Figure 8b shows a spectrum where the Doppler well is removed.

It is interesting to note that, in such graph, the corresponding Lamb dip to the transition  $|6^2s_{1/2}, F=4\rangle \rightarrow |6^2p_{3/2}, F'=4\rangle$  is highly overlapped with the crossover line. The overlap present on this experiment, but absent on the experiment of Sec. 2.2, comes from an increased linewidth originated by the corresponding increased power of the laser beams. Besides the power of the laser beams, there is another effect which is also increasing the transition linewidth. This is due to the frequency modulations on the laser beams used to obtain the dispersion-like signal. Frequency modulation also increases the frequency dispersion on the beams giving as a consequence the increased transition linewidth.

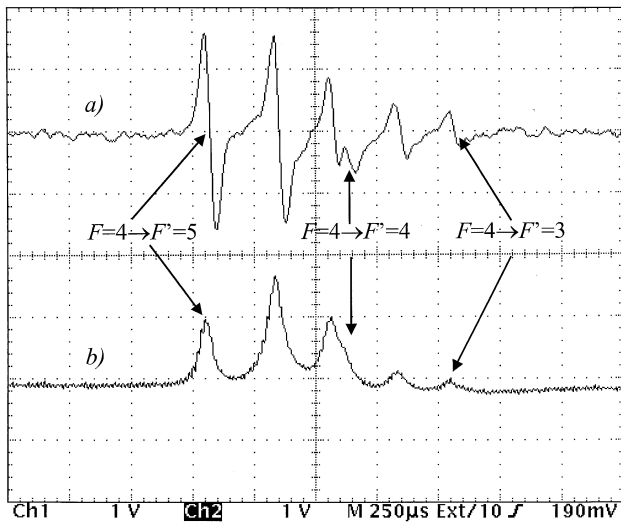


FIGURE 8. Experimental results of Cs-133 FM spectroscopy corresponding to the  $|6^2s_{1/2}, F = 4\rangle \rightarrow |6^2p_{3/2}, F' = 3, 4, 5\rangle$  transitions.

### 3.3. Dispersion-like signals without frequency modulation

The methods for generation of dispersion-like signals are based on the next approximation:

$$\frac{d}{d\omega} S(\omega) \propto \lim_{\delta\omega \rightarrow 0} [S(\omega + \delta\omega) - S(\omega - \delta\omega)]. \quad (5)$$

The dispersion-like signal is obtained from two spectrums slightly frequency shifted one respect to the other. In general terms, we can say that such frequency shifts are of around one half of the atomic transition linewidth. Those frequency shifts could be introduced using some physics phenomena such as the Zeeman effect [13,14], or the Doppler effect [15] among others.

#### 3.3.1. Dispersion-like signals using Zeeman effect

Figure 9 shows an experimental set up that could be used to generate a dispersion-like signal using the Zeeman effect. This set up is based on the saturation spectroscopy technique along with a longitudinal magnetic field. Such magnetic field brakes the degeneration at of the atoms hyperfine energy levels, in the gas. In Fig. 10, it is shown the Zeeman states of an hypothetical atom with two energy levels. Let's suppose that the quantum number  $F$  for the total angular momentum of the ground state, is zero, also and that  $F' = 1$  for the excited level. Under these conditions the quantum number  $m$ , corresponding to the projections of the total angular momentum, gets the value of  $m = 0$  for the ground state and  $m' = 0, \pm 1$  for the excited level.

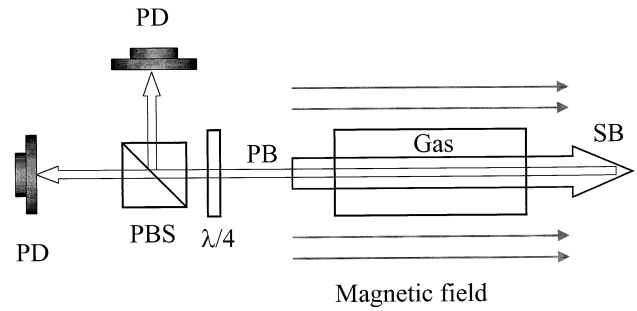


FIGURE 9. Experimental set up to generate dispersion-like signals using Zeeman effect. PD is a Photodetector, PBS is a Polarizing Beamsplitter,  $\lambda/4$  is a waveplate of  $\lambda/4$  retardation, PB is the Probe Beam, and SB is the Saturation Beam.

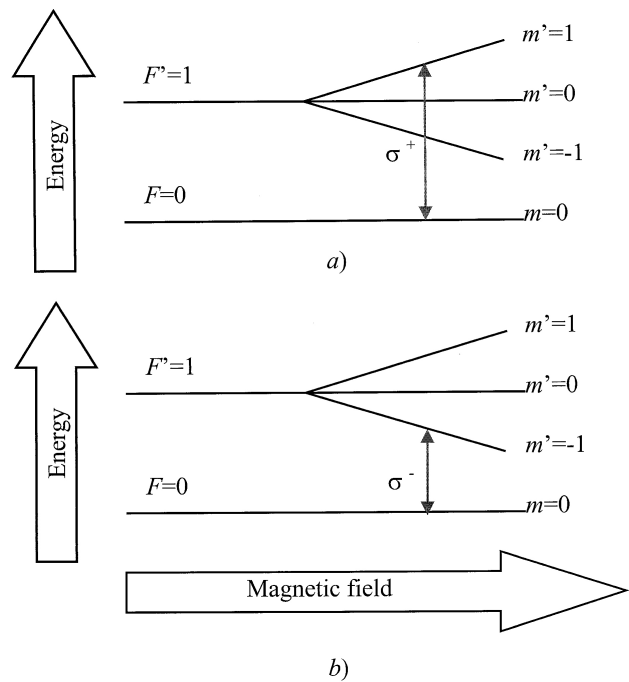


FIGURE 10. Zeeman levels of a fictitious two energy states atom. a) Atom interacting with a  $\sigma^+$  photon. b) Atom interacting with a  $\sigma^-$  photon.

Due to the geometry of this experiment, it is possible to have two energy spectrums shifted in frequency one respect to the other, if two light beams with circular polarizations ( $\sigma^+$  and  $\sigma^-$ ) are used. When an atom interacts with a  $\sigma^+$  photon, then the transition  $|F = 0, m = 0\rangle \rightarrow |F' = 1, m = 1\rangle$  occurs (see Fig. 10a), obtaining a blue shifted spectrum with respect to the transition  $|F = 0, m = 0\rangle \rightarrow |F' = 1, m = 0\rangle$ . On the other hand, the interaction with a  $\sigma^-$  photon induces the  $|F = 0, m = 0\rangle \rightarrow |F' = 1, m = -1\rangle$  transition (see Fig. 10b) obtaining, then, a red shifted spectrum with respect to the transition  $|F = 0, m = 0\rangle \rightarrow |F' = 1, m = 0\rangle$ . The detection of this two frequency shifted spectrums could be achieved by using a waveplate of  $\lambda/4$  retardation along with a polarizing beamsplitter. The dispersion-like signal is, then, obtained subtracting these two spectrums.

3.3.2. *Cs-133 spectroscopy and its application to the generation of dispersion-like signals using the Zeeman effect*

In this section, we consider the saturation spectroscopy in Cs-133 along with a longitudinal magnetic field (Zeeman effect). Figure 11 shows the experimental set up used to develop the conditions considered in this section. In this experiment, a cylindrical Cs-133 gas cell (2.5 cm in diameter and 4 cm long) was used under the same conditions as in Sec. 2.2. The longitudinal magnetic field was produced by a coil around the cell. Electric current through the coil was 200 mA, creating a constant magnetic field of around 0.35 mT at the middle part

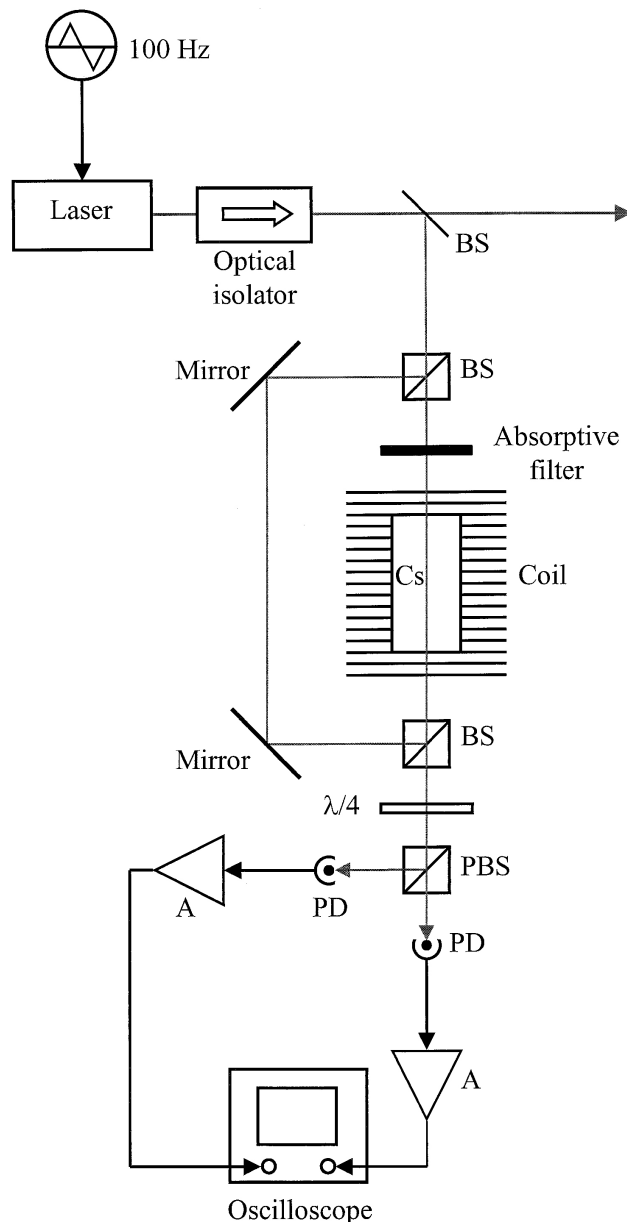


FIGURE 11. Schematic of the experimental set up to generate dispersion-like signals using the Zeeman effect on Cs-133. BS: Beamsplitter, PBS: Polarizing Beamsplitter, A: Amplifier, PD: Photodetector,  $\lambda/4$ : waveplate of  $\lambda/4$  retardation.

of the longitudinal axis of the cell. In order to get the polarization conditions ( $\sigma^+$  and  $\sigma^-$ ) on each laser beam, it was sufficient to polarize linearly each beam. This is valid because a linear polarization could be interpreted as the sum of  $\sigma^+$  and  $\sigma^-$  polarizations in the same strength. Power, diameter of saturation and detection laser beams were identical to those in Sec. 2.2.

The results obtained with this technique are shown in Fig. 12. The difference on these two spectrums was obtained using a digital oscilloscope. As expected, the spectrums get frequency shifted each one with respect to the other. That spectrum corresponds to the transitions  $|6^2s_{1/2}, F = 4\rangle \rightarrow |6^2p_{3/2}, F' = 3, 4, 5\rangle$ .

3.3.3. *Dispersion-like signals using Doppler effect*

It is possible to use the Doppler effect in order to get a frequency shift on the resonance spectrums. In Fig. 13a, we show an experimental set up for saturation spectroscopy, particularly one designed to use Doppler effect to get two resonance spectrums frequency shifted each one with respect to the other. In this case, the saturation and probe laser beams form an  $\theta$  angle between them. The intersection of this two laser beams occurs at the middle of the gas cell. Under these conditions, only those atoms that have the same Doppler frequency shift in both laser beams contribute to the spectrum (Lamb dip). The frequency shift due to Doppler effect is:

$$\omega - \omega_0 = \mathbf{v} \cdot \mathbf{k} = vk \cos \beta, \tag{6}$$

where  $\omega_0$  is the resonance angular frequency.

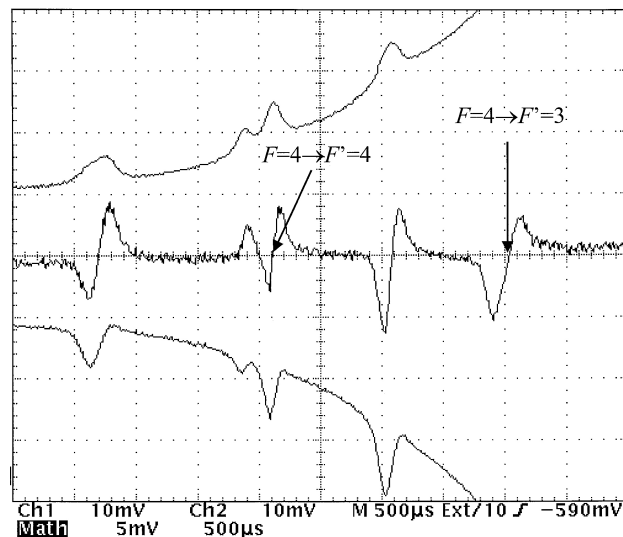


FIGURE 12. Dispersion-like signal obtained with the experimental set up showed in figure 11. The signals correspond to  $|6^2s_{1/2}, F = 4\rangle \rightarrow |6^2p_{3/2}, F' = 3, 4, 5\rangle$  transitions, where the zero crossing associated to  $|6^2s_{1/2}, F = 4\rangle \rightarrow |6^2p_{3/2}, F' = 3\rangle$  transition is not in view.

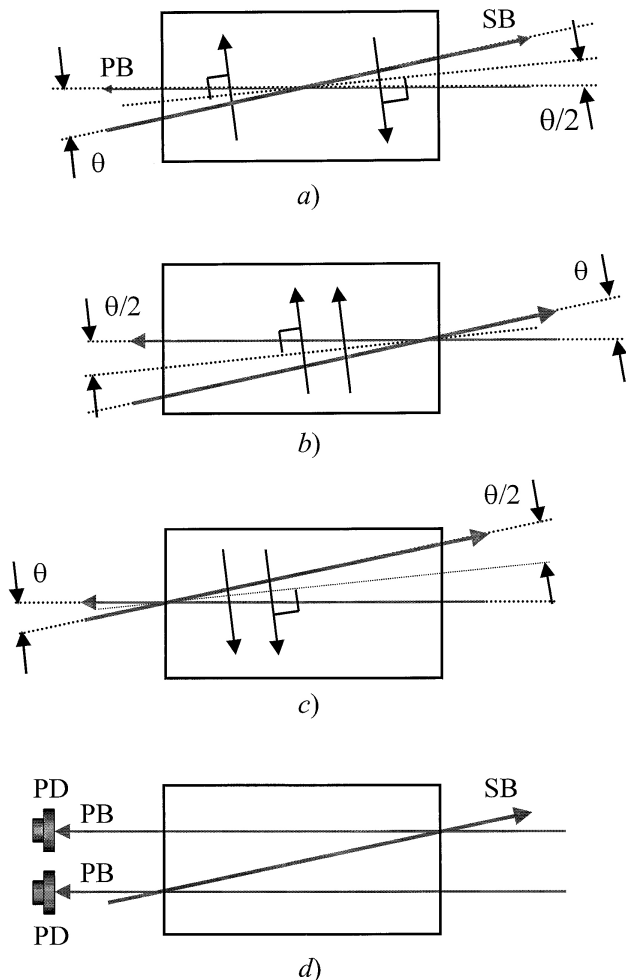


FIGURE 13. Generation of dispersion-like signals using Doppler effect. SB is the Saturation Beam, PB is the Probe Beam, PD is a Photodetector. a) The saturation and probe beam intersection is at the middle of the cell. b) and c) The intersection is at the extreme walls of the cell. d) Implementation of b) and c) cases simultaneously in the same experimental set up.

From Fig. 13a, it is possible to infer that when  $\beta$  angle is  $\pm(\pi - \theta)/2$ , then the previous conditions are satisfied. The atoms that move with this angle respect to the laser beams are represented with arrows in this figure. The spectrum obtained with the set up of Fig. 13a could be represented by the next equations [15]:

$$I(v) = A_- \int_{-\infty}^0 f(v)L(v - v_0 - \Delta v)dv + A_+ \int_0^{+\infty} f(v)L(v - v_0 - \Delta v)dv, \quad (7)$$

where:

$$f(v) = |v| \exp\left(-\frac{v^2}{v_m^2}\right), \quad (8)$$

$$L(v) = \gamma^2/(\gamma^2 + v^2), \quad (9)$$

with  $v_m = \sqrt{(2k_B T)/m}$ , where  $v_m$  is the most probable velocity,  $\gamma$  is the linewidth (half width at half maximum),  $\Delta v = (v/\lambda) \sin(\theta/2)$  is the frequency shift for an angle  $\theta$ , and  $v_0$  is the resonance frequency of the atom.

The coefficients  $A_-$  and  $A_+$  are related, respectively, to the blue and red shift by the Doppler effect. Such coefficients can be written as follows:

$$A_- = C_- \int_0^{I_x} \exp(-2\alpha l \tan(\theta/2))dl, \\ A_+ = C_+ \int_{I_x}^{I_0} \exp(-2\alpha l \tan(\theta/2))dl, \quad (10)$$

where  $C_-$  and  $C_+$  are constants,  $I_x$  is the position of the intersection of both light beams through the probe beam,  $\alpha$  is the saturation spectroscopy decay constant, and  $2l \tan(\theta/2)$  is the distance between the saturation and probe laser beams.

When the intersection of the laser beams is at the middle of the gas cell, as in Fig. 13a, then the coefficients  $A_-$  and  $A_+$  are equal, as it is shown in equation 10. On the other hand, when the intersection of the laser beams is at the wall cell position, as in Figs. 13b and 13c, only the atoms moving in an specific direction contribute to the absorption signal, and then one of the coefficients gets the value of zero. In such conditions, the resonance spectrum will be frequency shifted to blue (Fig. 13b) or to red (Fig. 13c).

When implementing these conditions in a single experimental set up, as shown in Fig. 13d, it is possible to obtain two resonance spectrums frequency shifted simultaneously each one with respect to the other. Finally, the dispersion-like signal is obtained subtracting both signals.

### 3.3.4. Cs-133 Spectroscopy and its application to the generation of dispersion-like signals using the Doppler effect

In Fig. 14, it is shown an schematic experimental set up implementing the technique for Cs-133 discussed in the previous section. In this case, a cylindrical Cs cell (2.5 cm in diameter and 7.5 cm in longitude) was used under the same temperature and pressure conditions as described in Sec. 2.2. The saturation beam, as well as the two probe beams, got the same characteristics in power and diameter as in the case discussed in Sec. 2.2. The distance between the two probe beams was 3.5 cm, with an angle of 2.67 degrees respect to the saturation beam. The dispersion-like signal obtained with this technique is shown in Fig. 15. It is important to notice that due to the very few electronic involved in this technique, there is a very good signal-to-noise ratio at the dispersion-like signal.

It is important to point out a comment on the dispersion-like signals obtained with the different methods discussed in this paper. Comparing the signal shown in Fig. 8a with the one shown in Fig. 15, and considering that both signals cor-



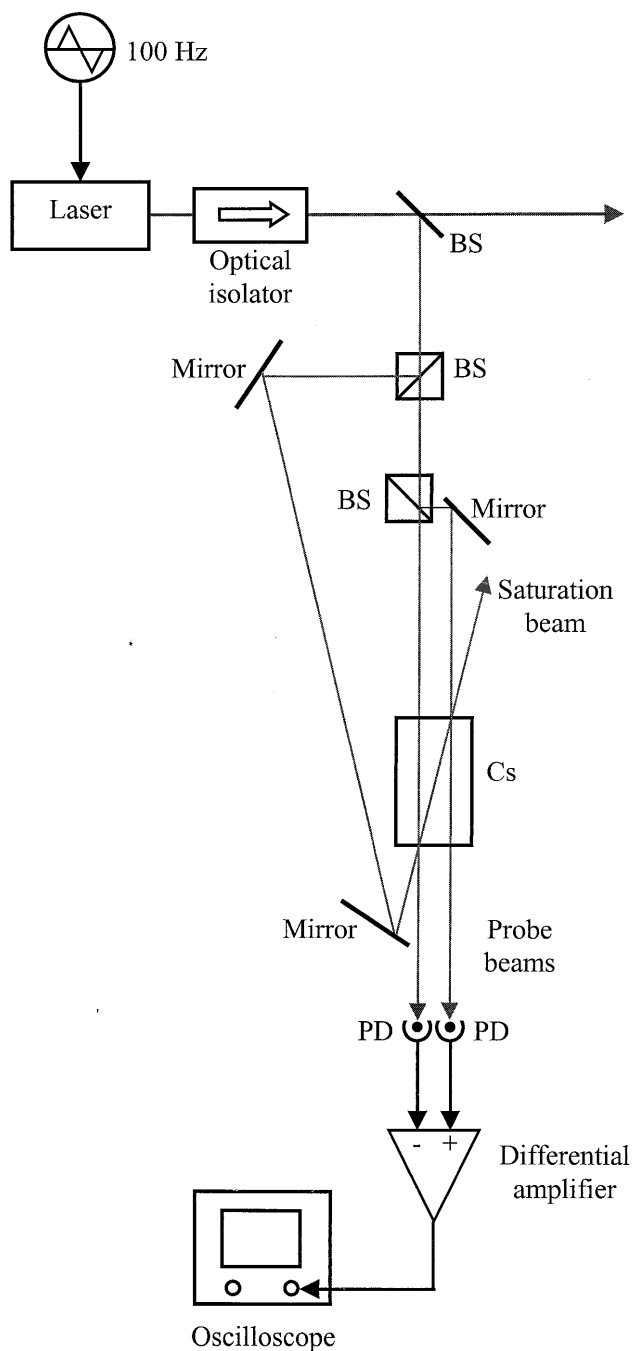


FIGURE 14. Schematics of the experimental set up to generate dispersion-like signals using Doppler effect on Cs-133. BS is a Beamsplitter and PD is a Photodetector.

respond to the same transition, there is a clear a difference between them. The most notable difference between them is on the relative strength of the Lamb deeps, and in consequence, on the dispersion-like signals. The differences on the Lamb deep strengths between spectrums are originated by the different longitude of the interaction paths involved in each experiment. In order to generate the signal shown in Fig. 8a, it was used an interaction longitude of around 1 cm, while in the generation of signal shown in figure 15 it was used an interaction longitude of around 7.5 cm.

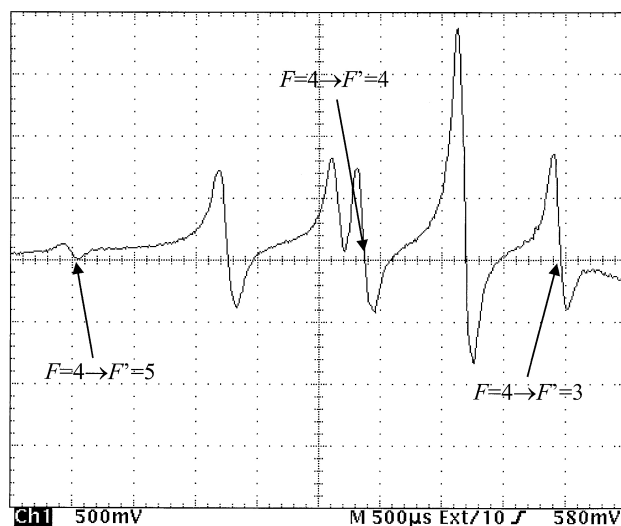


FIGURE 15. Dispersion-like signal generated with the experimental set up showed in Fig. 14. It is associated to  $|6^2s_{1/2}, F=4\rangle \rightarrow |6^2p_{3/2}, F'=3, 4, 5\rangle$  transitions.

When the laser is locked to the transition  $|6^2s_{1/2}, F=4\rangle \rightarrow |6^2p_{3/2}, F'=5\rangle$ , which is the one with highest probability, there will exist a maximum population of atoms at the Cs cell interacting with the laser beam. When the path length of the interaction is relatively small, lets say around 1 cm, then the attenuation of the laser beams is not too significant, and there will be a relatively strong signal at the detector, as shown in Fig. 8a. On the other hand, if the path length of the interaction is relatively large, lets say around 7.5 cm, the attenuation of the laser beams turns important and then the detector will receive a weak signal, as shown in figure 15.

Considering now the case when the laser is locked to the transition with the lowest probability, that is  $|6^2s_{1/2}, F=4\rangle \rightarrow |6^2p_{3/2}, F'=3\rangle$ . There is a minimum population of atoms at the Cs cell interacting with the laser beams. When the length of the path of interaction is large, lets say around 7.5 cm, the number of atoms interacting with the laser beam is also large enough to have a relatively strong signal at the detector, as shown in Fig. 15. On the other hand, when there is a short length of the path of interaction, lets say around 1 cm, there will be few atoms interacting with the laser beams and a weak signal at the detector, as shown in Fig. 8a.

#### 4. Conclusions

At normal conditions of pressure and temperature, there is a strong linewidth increment because the Doppler effect masks the atomic transitions. The technique known as saturation spectroscopy has the property to avoid such linewidth increment. In this paper, we discuss several methods to generate dispersion-like signals, such as frequency modulation (FM) spectroscopy, that is the most used technique to frequency stabilize semiconductor lasers. Other techniques that do not

use the FM were also reviewed, such is the case of those using the Zeeman effect and the Doppler effect.

We showed some results from the measurements of the Cs-133 spectrum using several methods discussed in this paper. The Doppler well appearing on the measured spectrums using the saturation spectroscopy technique induces systematic errors on the high accuracy measurement of the resonance frequencies. The elimination of the Doppler well on the spectrums also suppresses such systematic errors, which are of the order of magnitude of few Hz.

The path length of the interaction between atoms and

laser beams turns into an important factor on the generation of dispersion-like signals. The selection of the appropriate path length of such interaction highly improves the signal-to-noise ratio of the dispersion-like signal corresponding to the transitions with highest and lowest probability.

## Acknowledgements

Authors acknowledge to the Centro Nacional de Metrología, CENAM, for their support to develop this work.

- 
1. S. Chu, L. Hollberg, J.E. Bjorkholm, A. Cable, and A. Ashkin, *Phys. Rev. Lett.* **55** (1985) 48.
  2. C. Salomon, J. Dalibard, W.D. Phillips, A. Clarion, and S. Guellati, *Europhys. Lett.* **12** (1990) 683.
  3. E.A. Cornell and C.E. Wieman, *Reviews of Modern Physics* **74** (2002) 875.
  4. E.W. Hagley, L. Deng, W.D. Phillips, K. Burnett, and C.W. Clark, *Optics & Photonics News* (May 2001) 22.
  5. S.L. Rolston and W.D. Phillips, *Proceedings of the IEEE* **79** (1991) 943.
  6. T.W. Hänsch, M.D. Levenson, and A.L. Schawlow, *Phys. Rev. Lett.* **26** (1971) 946.
  7. V.S. Letokhov, *Saturation Spectroscopy in High-Resolution Laser Spectroscopy*, ed. by K. Shimoda, Chap. 4 Topics in Applied Physics, Vol 3 (Springer-Verlag, New York, 1976).
  8. C. Cohen-Tannoudji, J. Dupont-Roc, and G. Grynberg, *Atom-Photon Interactions* (John Wiley & Sons, Inc., New York, 1992).
  9. 13a. Conferencia General de Pesas y Medidas, 1967.
  10. D.A. Steck, *Cesium D Line Data* <http://george.ph.utexas.edu/~dsteck/alkalidata>.
  11. B. Pezeshki, *Optics & Photonics News* (May 2001) 34.
  12. L. Ricci *et al.*, *Optics Comm.* **117** (1995) 541.
  13. K.L. Corwin, Z.T. Lu, C.F. Hand, R.J. Epstein, and C.E. Wieman, *Appl. Opt.* **37** (1998) 3295.
  14. U. Shim, J.A. Kim, and W. Jhe, *J. Korean Phys. Soc.* **35** (1999) 222.
  15. S.E. Park, H.S. Lee, T.Y. Kwon, and H. Cho, *Optics Comm.* **192** (2001) 49.